Analysis of Urban Wind Turbines

J. Abraham, G. Mowry, and R. Erickson

University of St. Thomas, School of Engineering
2115 Summit Ave St. Paul, MN 55105-1079
jpabraham@stthomas.edu

ABSTRACT

A novel, vertical-axis wind turbine has been designed and analyzed for use in crowded urban and rooftop environments. The features of the turbine include a contoured blade which maximizes the rotational velocity while minimizing drag. The analysis of the device consisted of a two-step procedure which encompassed a fully three-dimensional simulation of the fluid flow around the blade and then a time-stepping procedure that allowed the determination of the rotational velocity of the turbine.

The calculations were carried out for wind velocities that ranged from 10 to 30 miles per hour. The resulting rotational velocity of the turbine was 137 revolutions per minute for wind velocities of 30 miles per hour. On the other hand, wind speeds of 20 and 10 miles per hour led to rotational velocities of 91 and 43 revolutions per minute, respectively.

When the entire set of results was assembled, it was possible to provide a simple expression which relates the rotational velocity to wind speed. This result will enable wind-power developers to predict the rotation and subsequent power generation from the turbine in advance of installation. The results indicate that this turbine design will generate appreciable electricity for local consumption.

Keywords: wind turbine, small-scale, vertical-axis, rooftop, urban

1 INTRODUCTION

A novel, vertical-axis wind turbine has been designed and analyzed. It is intended that this wind turbine will be suitable for applications in which the available space is constrained, such as on rooftops or in other urban situations. The vertical axis of the turbine provides a small footprint that is appropriate for such situations. These small wind turbines are able to generate local power for immediate use in the building or residence to which they are attached.

A depiction of the wind turbine is shown in Figure 1. There, the vertical axis of rotation is clearly shown in both the front, and top views. As can be seen in the figure, the two wind turbine blades consist of cupped surfaces located at the outboard ends of slender rods. On one side of the figure, the blade rotates with the wind whereas the rotation is opposite to the wind speed on the other side.

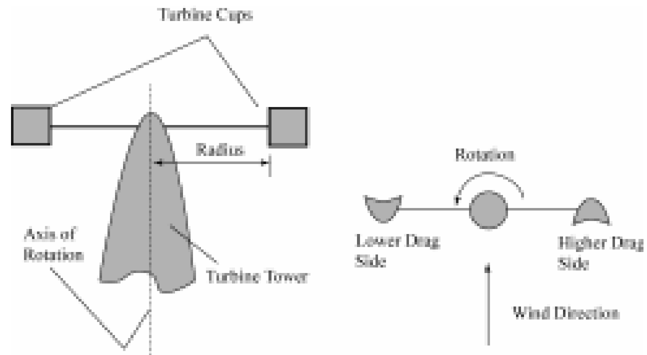

Figure 1: Schematic front and top views of the turbine.

2 NUMERICAL MODEL

The numerical model requires a calculation of the relative velocity of the incoming air stream. While the wind velocity was assumed to be steady in magnitude and direction (no gusts), the rotating motion of the turbine blade led to a continually changing relative wind velocity, as depicted in Figure 2.

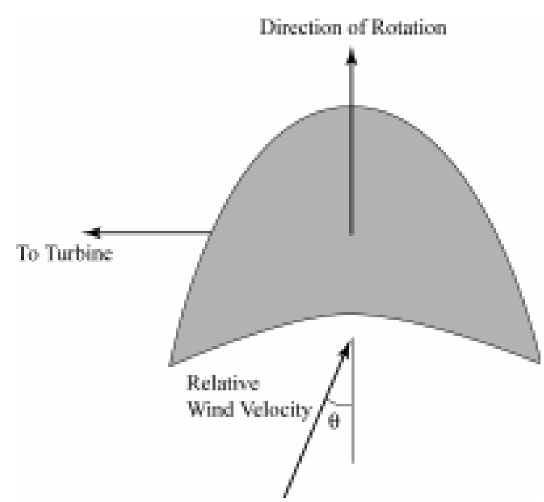

Figure 2: Diagram showing the incoming wind orientation. The angle θ varies continuously over a 360 degree range.

A diagram showing the boundary conditions which were used in the calculations is set forth in Figure 3. Also shown there are the dimensions of the turbine blade, as viewed from above. It was assumed that the wind passed parallel to the base of the wind turbine and did not spatially vary at the blade surface. The calculations were carried out for values of θ which spanned the entire 360° range. They also covered the expected range of relative wind velocities.

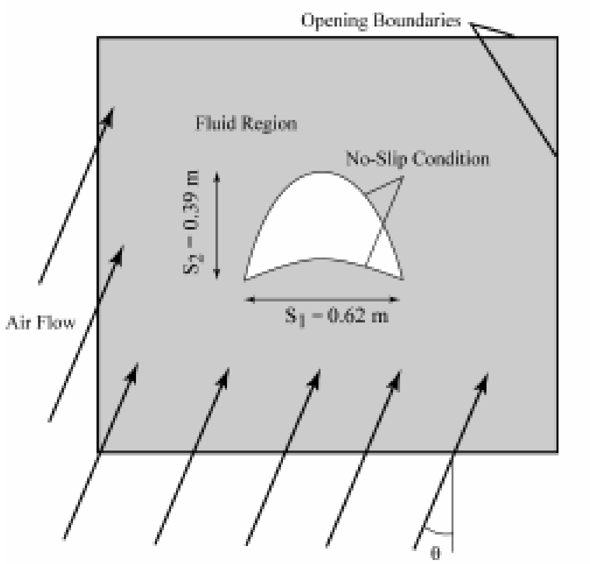

Figure 3: Boundary conditions used in the fluid simulation.

In order to complete the calculations, a control-volume numerical procedure was used. That method required that the entire region surrounding the turbine blade was subdivided into small calculations volumes (elements). Equations which govern conservation of mass, momentum, and turbulence were solved at each element of the assemblage. A depiction of the solution domain, subdivided by calculation elements is displayed in Figure 4. That figure shows the elements along a two-dimensional plane which passes horizontally through the turbine blade.

It can be seen from the figure that very small elements are deployed near the surface of the wind turbine to enable the resolution of the thin fluid boundary layer in that region. A callout is used in the figure to reinforce the small size of elements in the near-wall region.

2.1 Rotational Model

In order to calculate the rotational motion which results from the impinging wind, a force-moment analysis was carried out. That analysis utilized forces obtained from the solution to the fluid flow problem to determine an instantaneous angular acceleration of the turbine assembly. To assist with the description of the analysis, Figure 5 has been prepared. That figure shows a top view of the rotational turbine and two vectors which represent the respective circumferential forces. It can be seen from the figure that the two forces are expected to cause opposite moments about the turbine axis.

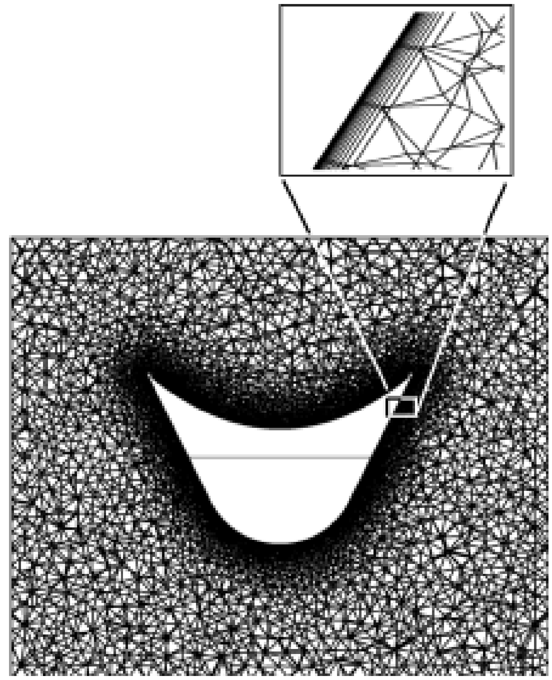

Figure 4: Fluid elements deployed throughout the air and in the region near the turbine-blade surface.

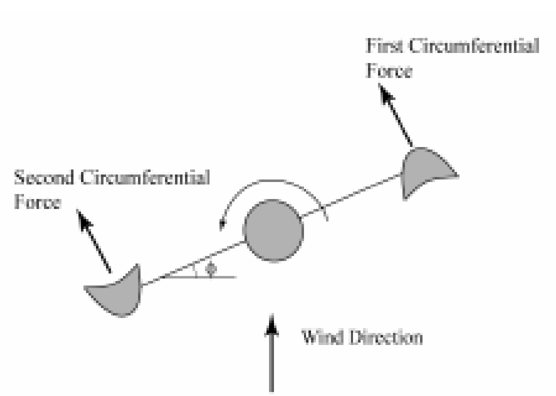

Figure 5: Schematic showing circumferential forces acting on the turbine blades.

With the two circumferential forces now determined, it is possible to describe the rotational motion of the turbine blade. The model relating the moments (M_1 and M_2) to the angular acceleration α is:

$$I\alpha = M_1 - M_2 = (F_1 - F_2) \cdot Radius \tag{1}$$

This model expressed in Eq. (1) does not include frictional forces within the turbine proper and, as a consequence, is an upper bound on the angular acceleration.

Clean Technology 2009, www.ct-si.org, ISBN 978-1-4398-1787-2

Forces F_1 and F_2 are, respectively, the forces promoting and opposing rotation. Both of these forces depend on the relative angles of the incoming wind and on the magnitude of the relative wind velocity, V_{rel}. If it is recognized that the instantaneous angular acceleration is the time derivative of the angular velocity, then Eq. (1) can be rewritten as

$$I\frac{d\omega}{dt} = \left(f\left(\theta_1, \left|V_{rel}\right|_1\right) - f\left(\theta_2, \left|V_{rel}\right|_2\right)\right) \cdot Radius \tag{2}$$

Where ω, the instantaneous angular velocity, is equal to

$$\frac{d\phi}{dt} = \omega \tag{3}$$

Here, ϕ is the angular position of the turbine arms as shown in Figure 5. The coupled set of equations (Eqs. (2) and (3)) can be solved in a time-stepping manner in which the change of angular velocity is determined at timestep n. From this information, the angular position of the turbine is determined at a following timestep $n + 1$. Mathematically, this two-step procedure is expressed in the following.

$$I\frac{d(\omega)^n}{dt} = \left(f\left(\theta_1, \left|V_{rel}\right|_1\right)^n - f\left(\theta_2, \left|V_{rel}\right|_2\right)^n\right) \cdot Radius \tag{4}$$

$$\phi^{n+1} = (\omega)^n \cdot \Delta t + \phi^n \tag{5}$$

and

$$(\omega)^{n+1} = (\alpha)^n \cdot \Delta t + (\omega)^n \tag{6}$$

Time steps were chosen to ensure accurate and stable solutions. The output of Eqs. (5) and (6) is used to update the wind speed and angle of incidence which then allow a determination of newly updated forces F_1 and F_2, and a continuation of the calculation procedure.

3 RESULTS AND DISCUSSION

As described in the foregoing, the solution procedure required that first, the solution for the flow patterns and circumferential forces were obtained for all possible wind speeds and directions. Then, the rotational motion of the turbine is obtained. The individual results of this two-step approach will now be described.

3.1 Fluid Flow Results

Although calculations were completed for a number of fluid velocities and directions, a representative selection of flow results will be shown here for brevity. To begin, Figure 6 has been prepared which displays the flow patterns that correspond to a relative angle of 0^o and a velocity of 20 miles per hour (9 meters/second). In the figure, fluid (moving downwards) impacts the concave surface of the turbine before being defected around the turbine blade. Large separation regions are evident on both sides of the blade.

A second display of flow patterns is shown in Figure 8. There, fluid is seen to impact the turbine blade at a relative angle of 60^o. Similar to Figure 7, these results also pertain to a relative wind speed of 20 miles per hour (9 meters/second). A distinct eddy is shown on the back-facing surface of the turbine blade. A unique feature is displayed in Figure 8 is a very low pressure zone to the lower-right side of the turbine blade. That low pressure region, which is a "lift" force on the turbine, actually aids in the rotational motion of the turbine assembly.

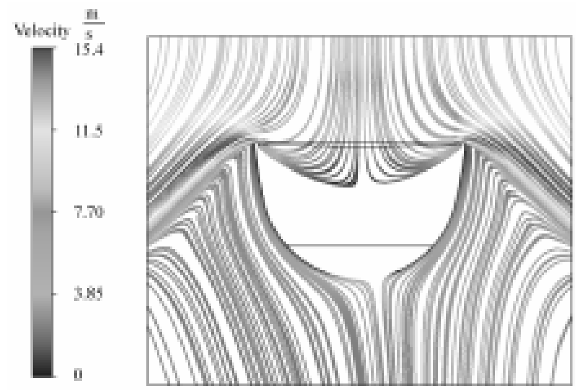

Figure 7: Streamline pattern for flow with an incident angle of 0 degrees, coded by velocity magnitude and corresponding to a relative wind speed of 20 miles/hour (9 m/s).

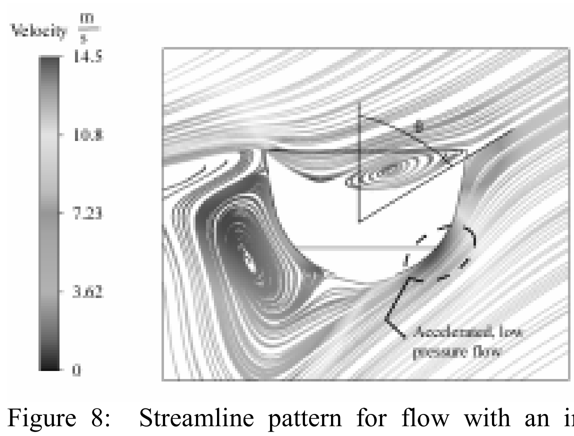

Figure 8: Streamline pattern for flow with an incident angle of 60 degrees, coded by velocity magnitude and corresponding to a relative wind speed of 20 miles/hour (9 m/s).

3.2 Rotational Results

With the flow field calculations completed and tangential forces now available, the numerical integration shown in Eqs. (5) and (6) can be completed. The calculations were carried out until the angular velocity of the turbine assembly was invariable from one cycle to the next. This quasi-steady result, here termed the *terminal angular velocity*, was obtained for wind speeds of 10, 20, and 30 miles per hour (4.5, 9.0, and 13.5 meters/second). A figure has been prepared which shows the variation of the terminal angular velocities for these three wind speeds. It may be noted that while there is some change in the angular velocity during a cycle, the conditions of quasi-steady state has been achieved. Figure 9 shows results for a full cycle of motion.

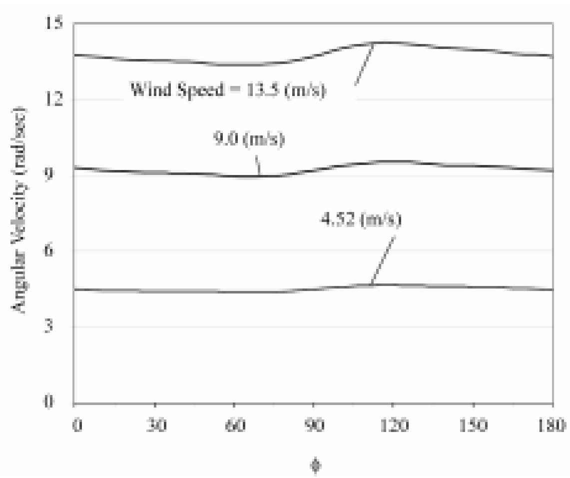

Figure 9: Values of the angular velocity for wind speeds of 4.52, 9.0, and 13.5 (m/s) which correspond, respectively, to 10, 20, and 30 miles/hour.

When the terminal velocity is obtained for a sequence of wind velocities, it is possible to develop a functional relationship between the two variables. Such a functional relationship is shown graphically in Figure 10.

The results of Figure 10 show that the terminal velocity depends nearly linearly on the magnitude of the wind speed. While this simple dependence may be unexpected, it must be recognized that for most of the rotational period, the opposing cups experience two counteracting forces. This fact tends to diminish the sensitivity of the angular velocity on the wind speed.

The final results, shown in Figure 10, can be used to predict an upper bound on the rotational motion of the vertical-axis turbine under consideration in this report. Furthermore, the dependence of the turbine performance with wind velocity is critical for the successful design of the overall system.

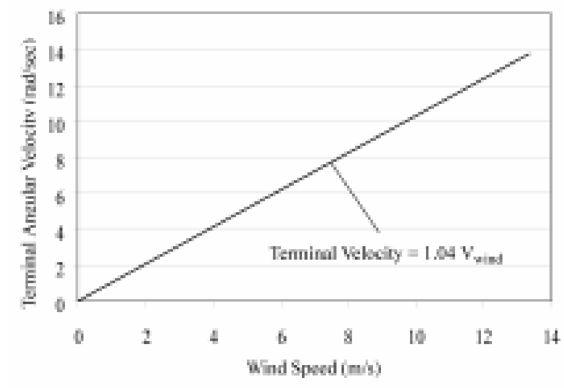

Figure 10: Variation of terminal velocity with wind speed.

4 CONCLUSION

A two-step solution approach has been described and carried out for the prediction of the performance of a small-scale, vertical-axis wind turbine that is suited for crowded urban environments, such as rooftops. The turbine has specially contoured, square profile cups that give rise to differing forces on their front and rear-facing surfaces. As a consequence, when placed in a steady air stream, a non-zero rotational motion results.

The model used here included a fully three dimensional solution of the fluid flow around the turbine blade. That fluid solution allowed the determination of forces which act on the blades at all instances in time. In turn, these forces could be used with a rotational model of the turbine. That model, which neglected friction forces, provides an upper bound on the rotational velocity of the turbine. The rotational velocity of the turbine varied slightly during any individual rotation but was steady when viewed on a cycle-by-cycle basis. The analysis allows the prediction of wind-turbine velocities for wind speeds other than those considered in this report.

Clean Technology 2009, www.ct-si.org, ISBN 978-1-4398-1787-2